Supporting Information for

Synthesis and Crystallization of Carboxylate Functionalized N-Heterocyclic Carbene-based Au_{13} Cluster with Strong Photoluminescence

Xiting Yuan,[a] Zichen Ye,[b] Sami Malola,[c] Osama Shekhah,[a] Hao Jiang,[a] Xinyan Hu,[b] Jian-Xin Wang,[a,d] Hong Wang,[d] Aleksander Shkurenko,[a] Jiangtao Jia,[a] Vincent Guillerm,[a] Omar F. Mohammed,[d] Xiaolan Chen,[b] Nanfeng Zheng,[b] Hannu Häkkinen,[c] Mohamed Eddaoudi[a*]

[a] Functional Materials Design, Discovery and Development Research Group (FMD[3]), Advanced Membranes and Porous Materials Center (AMPM), Division of Physical Sciences and Engineering (PSE), King Abdullah University of Science and Technology (KAUST), Thuwal 23955-6900, Saudi Arabia.

[b] State Key Laboratory for Physical Chemistry of Solid Surfaces, Collaborative Innovation Center of Chemistry for Energy Materials, and Department of Chemistry, College of Chemistry and Chemical Engineering, Xiamen University, Xiamen 361005, China

[c] Departments of Physics and Chemistry, Nanoscience Center, University of Jyväskylä, FI-40014 Jyväskylä, Finland

[d] Advanced Membranes and Porous Materials Center (AMPM), Division of Physical Sciences and Engineering (PSE), King Abdullah University of Science and Technology (KAUST), Thuwal 23955-6900, Saudi Arabia.

Contents

Synthesis and characterization:

1-Reagents.

$HAuCl_4$, Sodium Borohydride ($NaBH_4$), and dimethyl sulfide (Me_2S) were purchased from Sigma-Aldrich. Phenyl chloride was purchased from ACROS Organics. Methyl 1-benzylbenzoimidazole-5-carboxylate was purchased from Sungyoung Chemical Technology. Thiol-PEG5KDa-amine was purchased from Shanghai Ziqi biotechnology. 1, 2-Dibromopropane, hydrochloride acid (HCl) and N,N-Dimethylformamide (C_3H_7NO, A.R.), Diethyl ether ($C_4H_{10}O$), acetonitrile (CH_3CN) and methanol (CH_3OH) were purchased from VWR. The water used in all experiments was ultrapure. 4T1 cell line and L929 cell line were kindly provided by the Sun Yanan group, Department of Biomaterials, College of Materials, Xiamen University. Dulbecco's modified Eagle's medium (DMEM) was bought from Biological Industries, fetal bovine serum (FBS) was obtained from sigma Aldrich and penicillin–streptomycin was purchased from Thermo Fisher Scientific. All reagents were used as received without further purification. $AuSMe_2Cl$ was prepared according to literature methods.[1]

2-Synthesis:

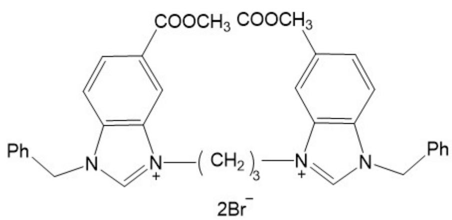

2.1 Synthesis of bi-NHC ester

In a 250 mL pressure vial, 1,3-Bis(Methyl 1-benzylbenzoimidazole-5-carboxylate)propane (1.3 g, 5 mmol) was dispersed in acetonitrile (50 mL). Then added with 1,3-Dibromopropane (495 µL). The mixture was reacted for 72 h at 90 °C. The resulting solution was dried under vacuum. Then add 5 mL acetonitrile to dissolve the product and added into 100 mL ether. The precipitate formed was filtered, washed with ether (2×5 mL), and dried in vacuum. Yield: 1.24 g (34.78%, based on 1,3-Bis(Methyl 1-benzylbenzoimidazole-5-carboxylate)propane). ^{1}H NMR (500 MHz, DMSO-d_6) d 10.39 (s, 2H), 8.68 (s, 2H), 8.12-8.21 (m, 4H), 7.58 (d, 2H), 7.44-7.37 (m, 6H), 5.88 (s, 4H), 4.85 (t, 4H), 3.93 (s, 6H), 2.73 (q, 2H). 13C NMR (500 MHz, DMSO-d6) d 165.7, 145.5, 134.3, 134.1, 131.9, 129.4, 129.2, 128.9, 127.6, 116.0, 114.9 ppm.

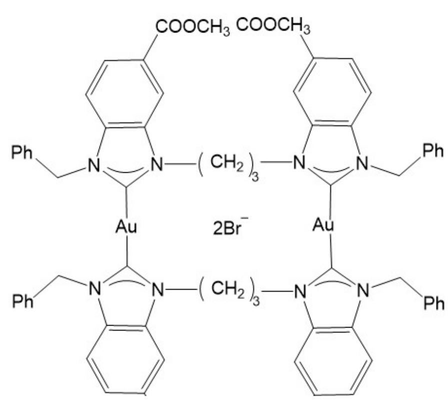

2.2 Synthesis of bi-NHC ester Au complex

Compound 1,3-Bis(Methyl 1-benzylbenzoimidazole-5-carboxylate)propane digold dibromide was prepared according to the literature.[2] A 50 mL pressure vial was charged with $AuSMe_2Cl$ (294.5 mg, 1 mmol), later, introduced the corresponding NHC ligand precursor 1,3-Bis(Methyl 1-benzylbenzoimidazole-5-carboxylate) propane dibromide (367mg, 0.5 mmol), $NaOAc{\cdot}3H_2O$ (3 mmol), and DMF (30 mL). The mixture was heated at 90 °C for 1.5 h. The resulting product was filtered. The solution was added dropwise into diethyl ether (100 mL), and the precipitate that formed was filtered, washed with water (2×10 mL), methanol/diethyl ether 1:4 (2×10 mL), and diethyl ether (2×10 mL), and dried under vacuum. Yield: 253.1 mg (22.63%, based on Au). ^{1}H NMR (500 MHz, $CDCl_3$) d 8.24 (s, 2H), 8.01 (d, 2H), 7.80 (d, 2H), 7.42-7.26 (m, 10H), 5.78 (s, 4H), 4.72 (t, 4H), 4.00 (s, 6H) 2.72 (q, 2H). ^{13}C NMR (500 MHz, $CDCl_3$) d 185.4, 166.0, 136.4, 134.2, 132.6, 129.1, 128.6, 127.6, 127.0, 126.4, 113.0, 53.5, 52.7, 45.7 ppm.

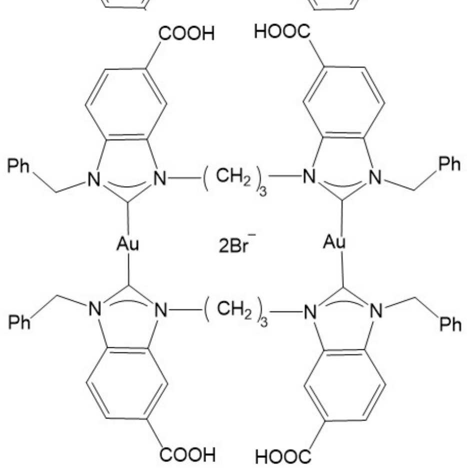

2.3 Synthesis of bi-NHC carboxyl Au complex

The synthesis of 1, 3-Bis (Methyl 1-benzylbenzoimidazole-5-carboxylate) propane digold dibromide was according to the method of Crudden.[3] In a 50 mL pressure vial, a mixture of 1,3-Bis(Methyl 1-benzylbenzoimidazole-5-carboxylate)propane digold dibromide (178 mg) and NaOH (40 eq) in EtOH-H_2O (1:1, 10 mL) was stirred at 90°C for 1 hour. Ethanol was removed in vacuo and the remaining aqueous solution was acidified to pH 1-2 by the addition of 2 N HCl. The precipitate was filtered and washed with H_2O (2×10 mL). Yield: 137.7 mg (80.1 %). ^{1}H NMR (500 MHz, CDCl3) d 8.44 (s, 2H), 8.09 (d, 2H), 7.47 (d, 2H), 7.40-7.32 (m, 10H), 5.87 (s, 4H), 4.78 (t, 4H), 2.92 (q, 2H). ^{13}C NMR (500 MHz, $CDCl_3$) d 180.8, 167.2, 135.9, 133.2, 129.2, 128.6, 127.7, 126.2, 114.3, 113.0, 52.2, 46.1, 30.1 ppm.

2.4 Synthesis and crystallization of Au_{13}-c cluster

The synthesis of Au_{13}(bi-NHC carboxyl)$_5Cl_2$ cluster was synthesized in one pot. In a typical synthesis, 8.2 mg (0.005 mmol) bi-NHC carboxyl Au complex was suspended in 1 mL H_2O. Later 20 eq NaOH was added. After stirring for 5 min, a clear solution was reached. Then added 10 equivalent $NaBH_4$ in 1 mL H_2O was added, during which the solution turns from brown to red. After 12 h, the suspension was filtered and of 20 µL HCl (12 M) was added to the supernatant, yielding red powder. The powder was washed with extra water (1×2 mL) and dried *in vacuo*.

Crystallization process: For the crystals, the powders were re-dissolved in 0.5 mL DMF and 5 eq HNO_3 (3 M, DMF). After one week in the 65 °C oven, red crystals were obtained. Modified crystallization process: the powders were dissolved in 0.5 mL DMF and $Cu(NO_3)_2$ (–COOH:Cu=1:1). After one week in the 65 °C oven, red crystals were obtained.

Figure S1. The photo of the crystals of Au_{13}-c cluster.

2.5 Modification of Au_{13}-c cluster with SH-PEG-NH_2

2 mg Au_{13}-c cluster and 20 mg SH-PEG-NH_2 (10 eq) were mixed in a 2 mL mixed solvent of ethanol and water (1:1). After stirring for 12 h, the mixture was washed with acetone, after centrifugation, the obtained material of Au_{13}+PEG was dissolved in 1 mL water or Dulbecco's Modified Eagle Medium (DMEM) for further use.

Single-crystal X-ray diffraction (SCXRD) Analysis: Single Crystal X-ray Diffraction data were collected using Bruker X8 PROSPECTOR APEX2 CCD diffractometer using CuKα radiation (λ = 1.54178 Å). Indexing was performed using APEX3[4a] v2018.7-2 (Difference Vectors method). Data integration and reduction were performed using SaintPlus (Bruker AXS. Inc, Madison, Wisconsin, USA, 2018) 8.38A. Absorption correction was performed by the multi-scan method implemented in SADABS-2016/2.[4b] Space group was determined using XPREP implemented in APEX3.[4c] The structure was solved using Direct Methods

(SHELXS-2008)[5] and refined using SHELXL-2018/3[6] (full-matrix least-squares on F^2) contained OLEX2 program[7] package. More details about crystal data and structure refinement are shown in Table S1.

The crystal was realized to be sensitive to X-ray radiation which reduces the collected data resolution from 0.84 Å to 0.87 Å and the radiation damage has been taken into account during the data scaling and absorption correction. Due to poor diffraction, a set of restraints and constraints was applied to make both geometry and ADPs of the organic ligands reasonable (DFIXes for 1, 2- and 1, 3-interatomic distances). The planarity of the moieties with sp2 C atoms was reached by FLAT.

Thus, $C_{carbene}$–N and N–$C_{aromatic}$ bond lengths were restrained to 1.36 and 1.39 Å. The geometries of the benzene rings were constrained by AFIX 66. Single $C_{aromatic}$–$C_{carboxylate}$ bond lengths were restrained to 1.50 Å. Two carboxylic groups were found to be fully deprotonated. C–O Bonds of the deprotonated carboxylates were restrained to 1.26 Å, whereas the double C=O and the single C–O (H) bonds of the carboxylic groups were restrained to 1.21 and 1.30 Å. Single N–C bonds were restrained to 1.43 Å. Single C–C bonds were restrained to 1.51 Å. The directionality of the single bonds was restrained by SADI. The 1, 3-distances in the propylene chains were restrained to 2.47 Å. Anti-bumping restraints DFIX -2.7 to prevent too close O···O contacts were applied between the couples O2A/O2W and O8A/O4W. ADPs of the organic ligand atoms were restrained by SIMU. ADPs of closely located couples of N2A/N6A, N3A/N7A, N4A/N8A, and N1A/N5A were constrained to be the same.

Additionally, to two fully deprotonated carboxylic groups, 68% of carboxylic group C8A is deprotonated and coordinated by $Na(H_2O)_3$; this also caused a disorder of the whole ligand A over two positions. The occupancy was refined first free to 0.683(7) and then fixed at 2/3. The distances Na–O and ADPs were restrained to be similar and ADPs of Na1/O3W atoms were constrained to be the same. ADPs of Na1, O1W, O5W, O6W, and O8W were restrained to be close to isotropic (ISOR). Hydrogen atoms were placed at the calculated positions and refined using a riding model with $U_{iso}(H) = 1.2U_{eq}(C)$ or $1.5U_{eq}(O)$.

The uninterpretable electron density was found in the voids in the structure and masked from the refinement using the SQUEEZE routine implemented in the program PLATON: the structure factors were augmented via reverse Fourier transform methods.[7] The resultant FAB file containing the structure factor contribution from the electron content of the void space was used together with the original HKL file in further refinement. The FAB file with details of the SQUEEZE results is appended to this CIF file. The SQUEEZE procedure corrected for 4639 electrons within the solvent-accessible voids (total of 10875 Å^3).

It was not possible to localize all H-atoms in the structure from the single crystal data, but the reported formula includes them. The final crystallographically estimated formula of the **Au$_{13}$-c** material is $H_{6.33}[Na(H_2O)_3]_{0.67}[Au_{13}(C_{33}H_{26}N_4O_4)_5Cl_2)]\cdot 2.42(H_2O)\cdot x(solv)$.

The X-ray crystallographic data for **Au$_{13}$-c** has been deposited at the Cambridge Crystallographic Data Centre (CCDC), under deposition number 2249862. These data can be obtained free of charge from the CCDC via www.ccdc.cam.ac.uk.

Table S1. Crystal data and structure refinement for **Au_{13}-c**

Empirical formula	$C_{165} H_{145.17} Au_{13} Cl_2 N_{20} Na_{0.67} O_{24.42}$
Formula weight	5445.71
Crystal system, space group	Monoclinic, $P2_1/n$
Unit cell dimensions	a = 26.064(1) Å
	b = 27.538(1) Å, β = 91.118(2)°
	c = 35.319(1) Å
Volume	25345(2) Å^3
Z, calculated density	4, 1.427 Mg m^{-3}
F(000)	10156
Temperature (K)	100.0(1)
Radiation type, λ	Cu $K\alpha$, 1.54178 Å
Absorption coefficient	14.34 mm^{-1}
Absorption correction	Multi-scan
Max and min transmission	0.099 and 0.016
Crystal size	0.05 × 0.06 × 0.06 mm
Shape, colour	Prism, red
θ range for data collection	3.8–65.9°
Limiting indices	$-30 \le h \le 30$, $-31 \le k \le 32$, $-40 \le l \le 36$
Reflection collected / unique / observed with $I > 2\sigma(I)$	291486 / 41296 (R_{int} = 0.062) / 28907
Completeness to θ_{full} = 62.4°	98.0 %
Refinement method	Full-matrix least-squares on F^2
Data / restraints / parameters	41296 / 2655 / 2095
Final R indices [$I > 2\sigma(I)$]	R_1 = 0.062, wR_2 = 0.186
Final R indices (all data)	R_1 = 0.081, wR_2 = 0.218
Weighting scheme	$[\sigma^2(F_o^2) + (0.1224P)^2 + 69.4463P]^{-1*}$
Goodness-of-fit	1.03
Largest diff. peak and hole	1.14 and -1.83 e Å^{-3}

$^*P = (F_o^2 + 2F_c^2)/3$

3-Characterization

3.1 Physical Measurements.

UV−Vis absorption spectra were recorded on a Cary 5000 UV-Vis-NIR spectrophotometer and emission properties were measured on a Fluotomax-4 spectrophotometer using a quartz cuvette of 1 cm path length. The photoluminescence quantum yield (PLQY) of the samples was measured using an FS5 fluorescence spectrometer (Edinburgh Instruments). The excitation wavelength was set at 420 nm. Mass spectra were recorded on an apex-Ultra FTICR-MS. The ^{1}H&^{13}C NMR spectra were recorded on a Bruker AVANCE III 500 MHz spectrometer in DMSO-d_6 and $CDCl_3$. Chemical shifts are reported in ppm with the internal tetramethylsilane signal at 0.0 ppm as a standard. IR spectra were recorded on a Fourier transform infrared spectrometer (Nicolet iS50, Thermo Fisher Scientific Inc., USA).

3.2 Stability studies for Au_{13}-c cluster:

3.2.1 Ox-red stability studies.

$NaBH_4/H_2O$ solution of **Au_{13}-c** was treated with a 1.8 M H_2O_2 aqueous solution or 0.02 mM $NaBH_4$ aqueous solution. The samples were characterized by UV-Vis spectra during the period of 12 h.

3.2.2 pH stability studies.

The **Au_{13}-c** samples were treated with 12 M HCl or 181.44 mg/mL NaOH to adjust the pH of the solution to be 1, 4, 7, 11, and 14, respectively. The solution was kept at room temperature. The samples were then characterized by UV-Vis spectroscopy during the period of 12 h.

3.2.3 Glutathione (GSH) stability study.

Crystals of **Au_{13}-c** were dissolved in 2 mM and 10 mM L-glutathione aqueous solution. The solution was kept at room temperature. The samples were then characterized by UV-Vis spectroscopy during the period of 12 h.

3.2.4 Electrolyte stability studies.

The **Au_{13}-c** sample was dissolved in 150 mM NaCl aqueous solution. The solution was kept at room temperature. The samples were then characterized by UV-Vis spectroscopy during the period of 12 h.

3.2.5 Thermal stability studies.

The **Au_{13}-c** sample was dissolved in NaOH aqueous solution (pH=14). The temperature of the solution was rising from room temperature to 45 ºC, 65 ºC, 85 ºC, and finally to 105 ºC. Every temperature was kept for ten minutes. The samples were characterized by UV-Vis spectroscopy during the period.

3.2.6 Quantum yields tests of Au_{13}-c cluster

The crystals of the Au13-c cluster were first dissolved in NaOH aqueous solution and then precipitated with HCl solution. The resulting product was used to dissolve in DMF or disperse in water for the quantum yield (QY) test.

4-Computational Methods

Density functional theory (DFT) was used for the calculations as implemented in the software GPAW.[9] GPAW uses real-space grids and scalar-relativistic corrections for the setups of metal atoms. The crystal structure of $[Au_{13}(\text{bi-NHC carboxyl})_5Cl_2]^{3+}$ cluster was used as a starting structure for calculations. All carboxylic groups were protonated. The cluster was first optimized using a 0.2 Å real-space grid and Perdew-Burke-Ernzerhof (PBE) xc-functional.[10] Convergence in optimization was expected to be reached when the maximum forces of the atoms were below 0.05 eV/Å. Electronic structure was analyzed by projecting the density of states to spherical harmonics functions centered at the center of the mass of the cluster using a cut-off radius of 12.5 Å.[11] This analysis can reveal the symmetries of the superatom states delocalized in the metal core and also give information on where the ligand states are. Optical absorption spectra were calculated using linear response time-dependent density functional theory (lr-TDDFT)[12] and PBE functional as a kernel. The features of the optical absorption spectra were analyzed by solving so-called dipole transition contribution maps (DTCM) using time-dependent density functional perturbation theory.[13] DTCM reveals the strengthening and screening contributions to the total transition contribution map as decomposed to Kohn-Sham basis. It can be used to assign the origin of the absorption features to different parts of the structure for example by plotting DTCM with respect to the localization of the electron states.

5-The MTT assay

The cytotoxicity of Au_{13}-PEG against 4T1 and L929 cell lines was tested following the standard 3-(4,5-dimethylthiazol-2)-2,5-diphenyltetrazole bromide (MTT) assay. After incubation for 24 h, cells were seeded into a 96-well plate with a density of $1×10^4$ and cultured for another 12 h. Then the Au_{13}-PEG (in DMEM) of different concentrations were added into each well. Each concentration was represented by 5 replicate wells. After 12 h, 100 µL of MTT reagent (0.5 mg·mL^{-1}) was added into each well after removing the original drug and then carrying out another 4 h-co-incubation. Finally, sucked out the MTT solution and put 150 µL of DMSO into each well Dual wavelength absorbance was measured on a Tecan infinite M100 microplate reader (the measurement and reference wavelengths were 570 nm and 490 nm respectively. Relative cell viability (%) was calculated according to the following formula:

Cell viability (%) = (the mean of absorbance of a treatment group / the mean of absorbance of the control group) × 100%

5.1 The cellular staining capacity of Au_{13}-PEG

Confocal laser scanning microscopy (CLSM) was employed to evaluate the ability of Au_{13}-PEG to stain the two cell lines (4T1 and L929). The living cells were incubated with glass bottom culture dishes in DMEM containing 10% FBS. When the cells' confluence reached 60%, they were washed 3 times with PBS and fully replaced the culture media with 75 µg·mL^{-1} Au_{13}-PEG (in DMEM). Then, remove the nutrient solution after 24 h or 48 h incubation. And the staining situation was observed by CLSM (excited wavelength: 488 nm, emission wavelength: 650 nm-750 nm) after washing the culture dishes with PBS thrice. In addition, the cell nuclear was stained with Hoechst 33342 (excited and emission wavelengths were at 405 nm and 461 nm).

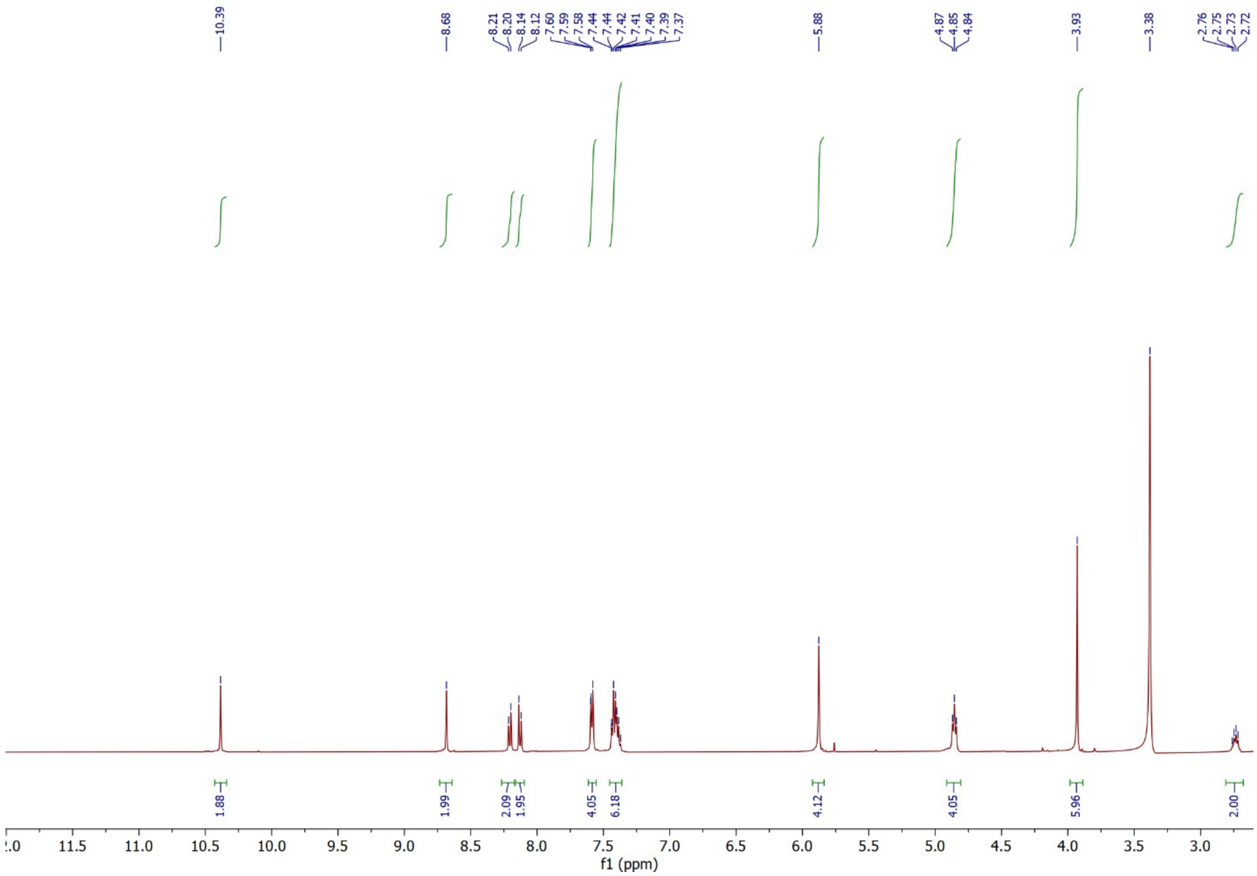

Figure S2. ^{1}H NMR spectrum of bi-NHC ester in d_6-DMSO

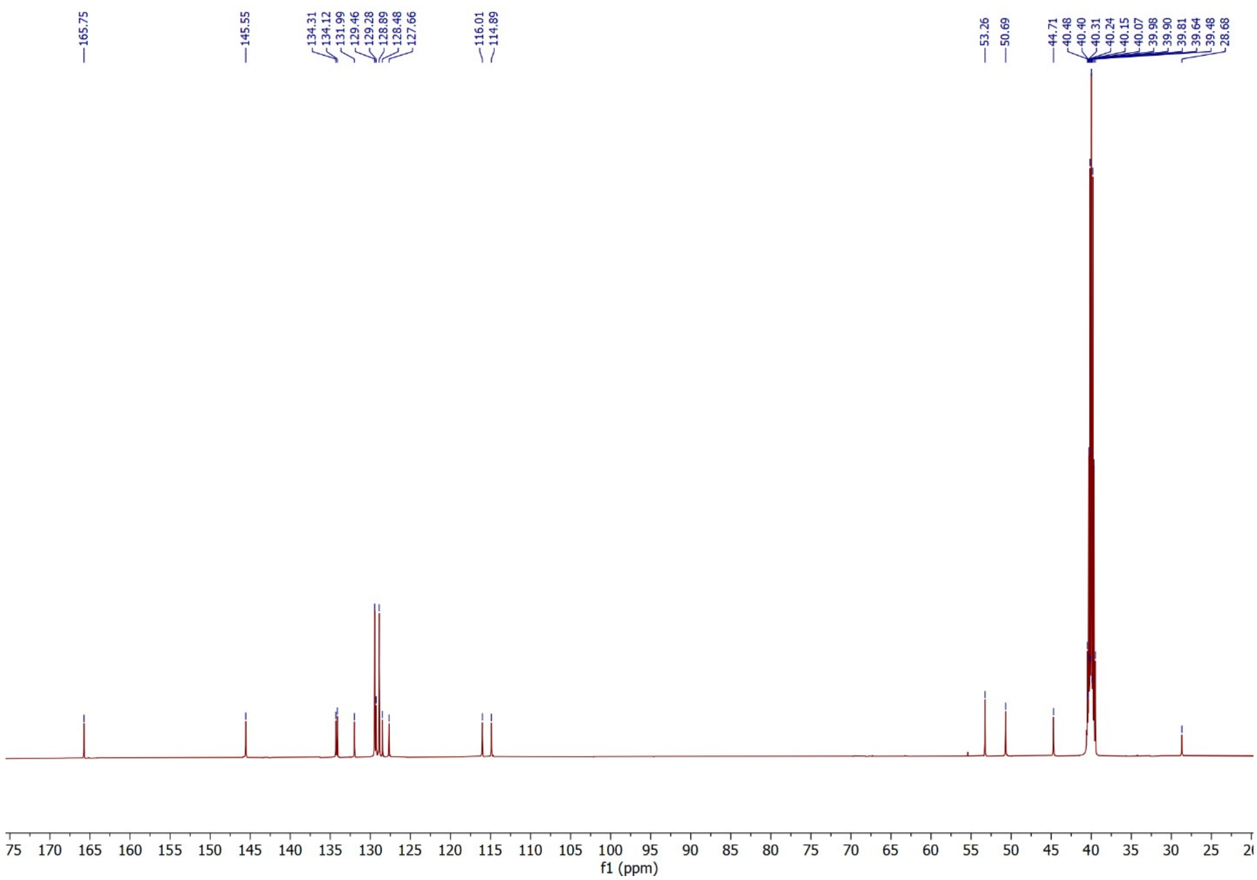

Figure S3. ^{13}C NMR spectrum of bi-NHC ester in d_6-DMSO

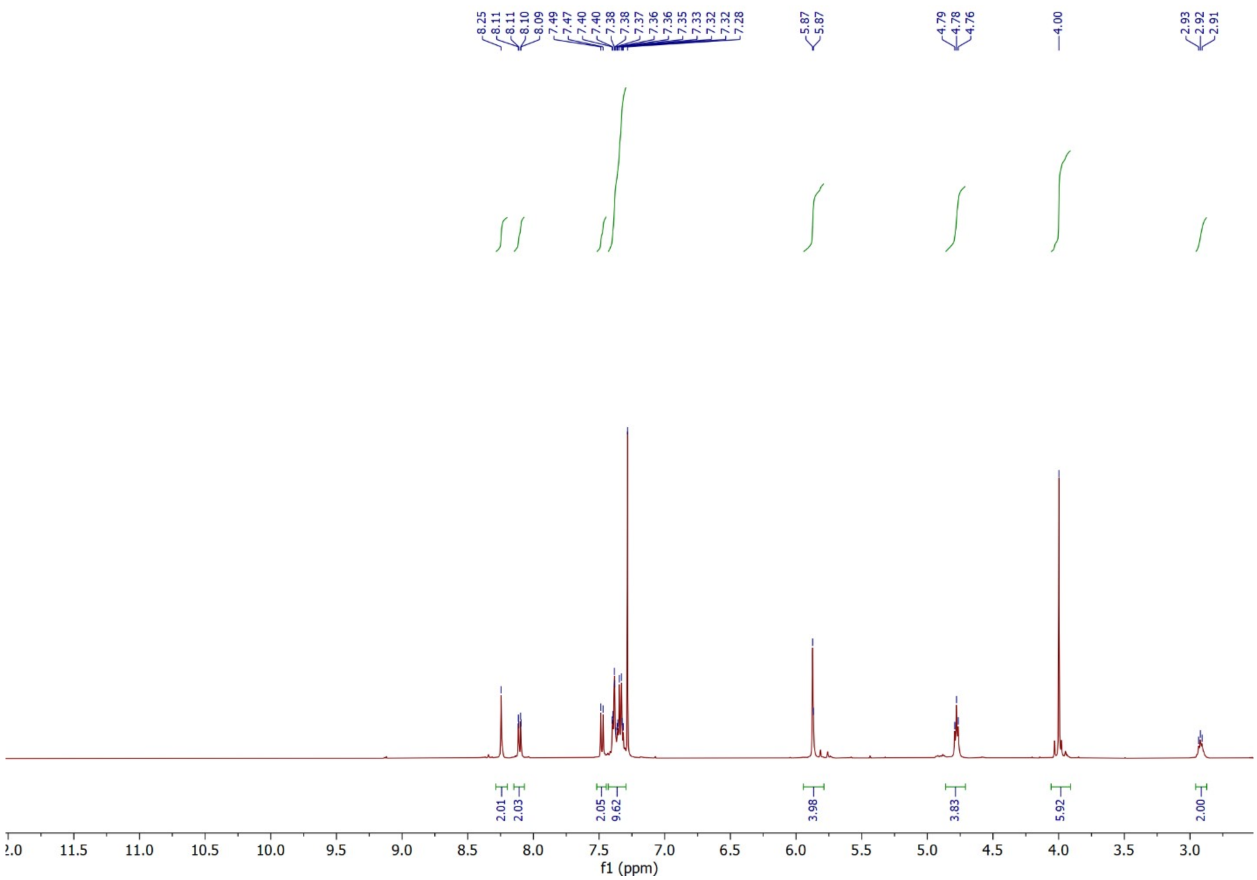

Figure S4. ^{1}H NMR spectrum of bi-NHC ester Au in d-$CHCl_3$

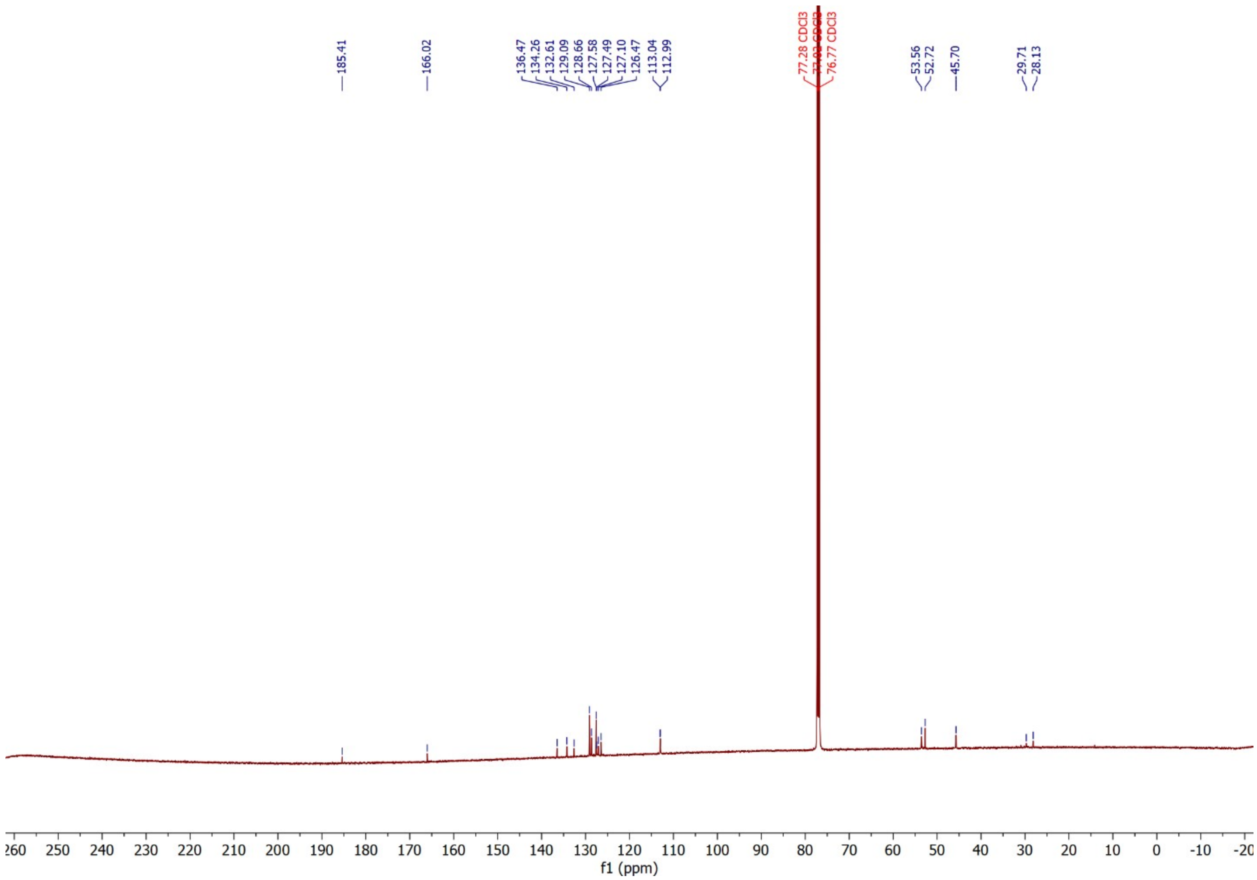

Figure S5. ^{13}C NMR spectrum of bi-NHC ester Au in d-$CHCl_3$

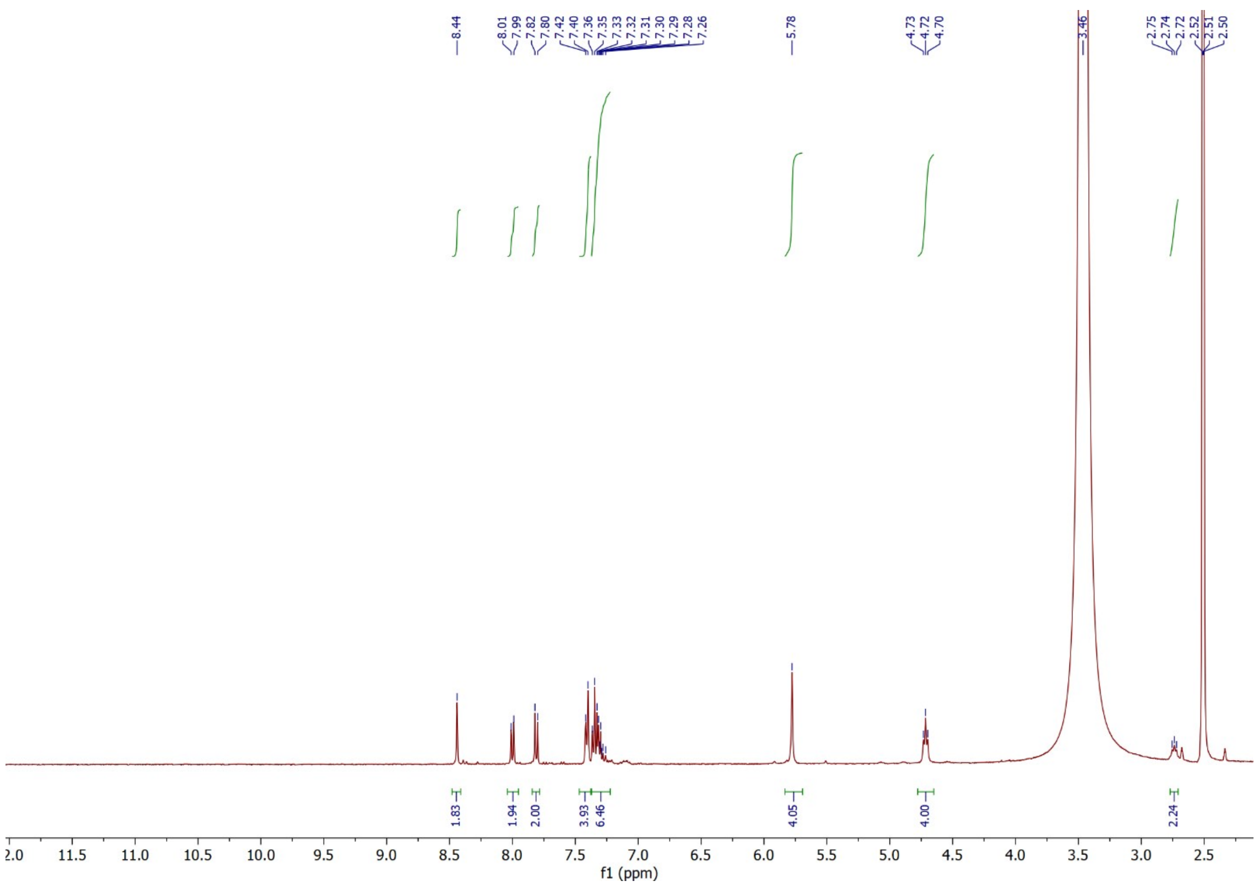

Figure S6. ^{1}H NMR spectrum of bi-NHC carboxyl Au in d_6-DMSO

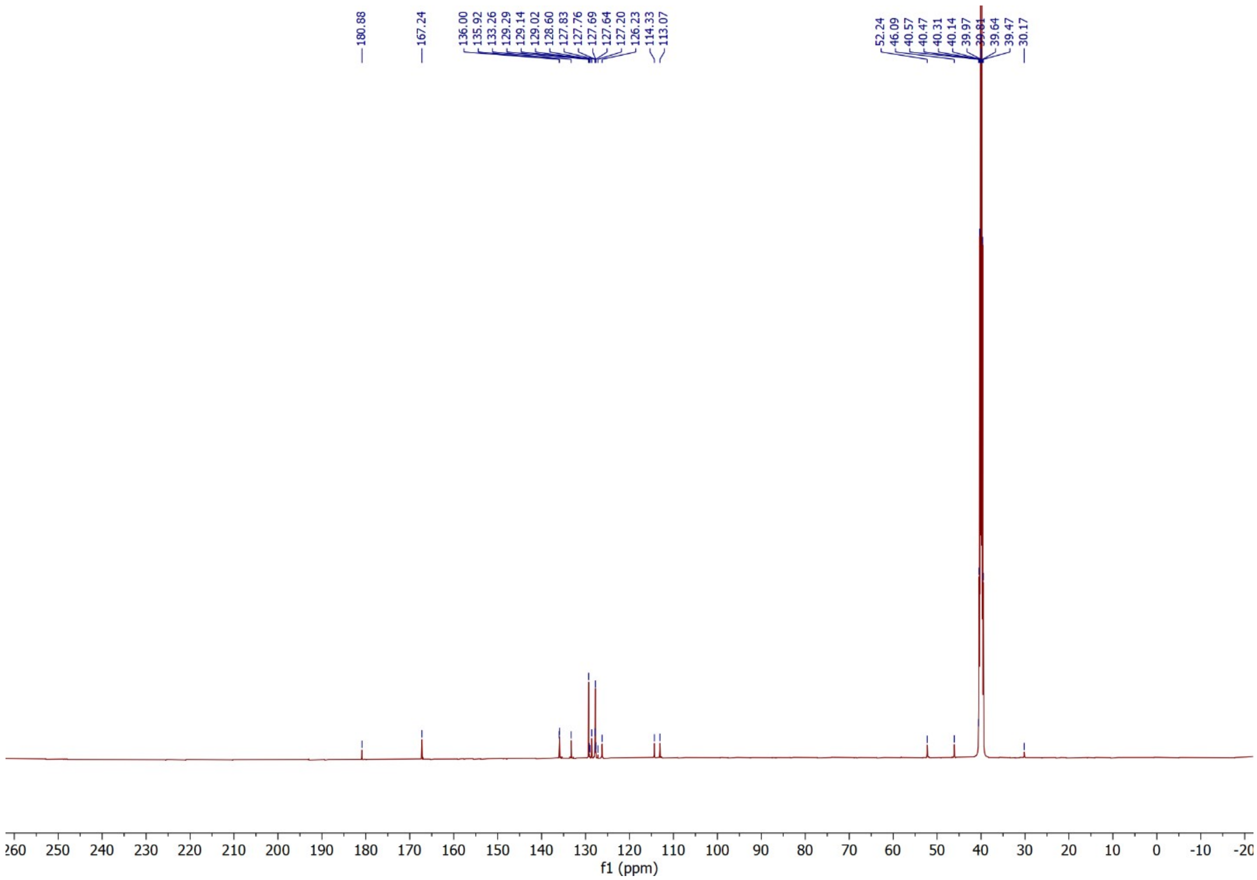

Figure S7. ^{13}C NMR spectrum of bi-NHC carboxyl Au in d_6-DMSO

Table S2: Comparison of bi-NHC protected Au_{13} NCs

Average distances	Au_{Core}-Au_{Shell} (Å)	Au_{Core}-Au_{C} (Å)	Au_{Core}-Au_{Hal} (Å)	Reference
Au_{13}(bi-NHC1)$_5$$Br_2$	2.76(2)	2.77(1)	2.726(8)	14
Au_{13}(bi-NHC2)$_5$$Cl_2$	2.77(2)	2.77(1)	2.74(1)	15
Au_{13}(bi-NHC3)$_5$$Br_2$	2.77(3)	2.78(2)	2.727(4)	16
Au_{13}(bi-NHC4)$_5$$Br_2$	2.78(3)	2.79(1)	2.725(4)	16
Au_{13}(bi-NHC5)$_5$$Br_2$	2.78(3)	2.78(3)	2.739(7)	16
Au_{13}-c	2.75(2)	2.758(6)	2.721(2)	This work

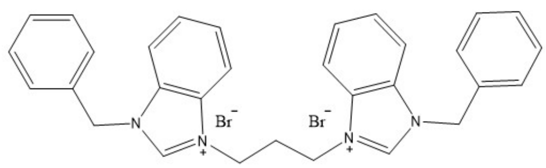

bi-NHC1

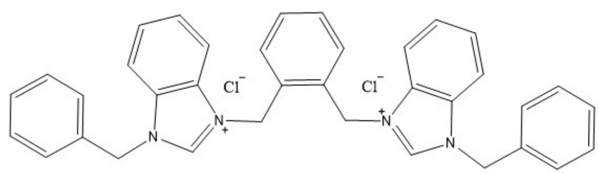

bi-NHC2

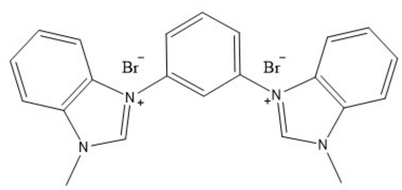

bi-NHC3

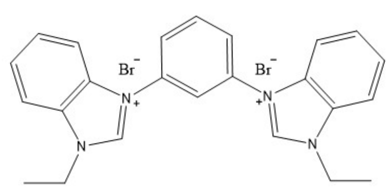

bi-NHC4

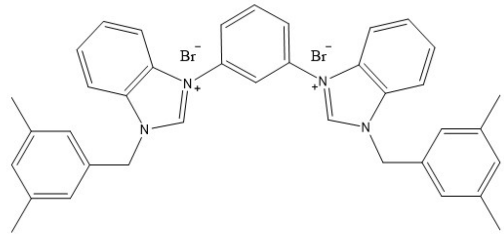

bi-NHC5

Table S3. Interactions C–H⋯Au in **Au_{13}-c**

C–H⋯Au	*d*(C–H), Å	*d*(H⋯Au), Å	*d*(C⋯Au), Å	∠(C–H⋯Au), °
C19A–H19A⋯Au5	0.99	2.75	3.36(2)	119
C20–H20A⋯Au4	0.99	2.69	3.33(2)	123
C20C–H20E⋯Au8	0.99	2.84	3.41(1)	118
C20E–H20I⋯Au12	0.99	2.81	3.40(1)	119
C27C–H27E⋯Au9	0.99	2.82	3.42(1)	120
C27D–H27G⋯Au11	0.99	2.80	3.40(1)	120
C27E–H27I⋯Au13	0.99	2.85	3.44(2)	119
C48A–H48A⋯Au4	0.99	2.76	3.38(5)	121
C58A–H58A⋯Au5	0.99	2.84	3.45(5)	120

Table S4. Interactions C–H⋯π in **Au_{13}-c**

C–H⋯π	*d*(H⋯Cg), Å	∠(C–H⋯Cg), °	*d*(C⋯Cg), Å	*d*(H⋯π), Å	∠(C–H⋯π), °
C20B–H20D⋯π_{21A}	2.84	134	3.61(2)	2.65	115
C20C–H20F⋯π_{21B}	2.98	128	3.68(2)	2.78	125
C22A–H22A⋯$\pi_{1A'}$	2.98	121	3.57(3)	2.47	178
C22C–H22C⋯π_{1C}	2.99	117	3.52(1)	2.51	178
C22D–H22D⋯π_{1D}	2.98	118	3.54(1)	2.47	176
C33A–H33A⋯π_{9A}	2.98	118	3.52(3)	2.50	176
C33D–H33D⋯π_{9D}	2.99	118	3.54(1)	2.45	174
C53A–H5⋯π_{1A}	2.64	126	3.29(4)	2.28	173
C53A–H53A⋯$\pi_{1A'}$	2.38	127	3.05(4)	2.19	165
C64A–H64A⋯π_{9A}	2.74	116	3.27(4)	2.57	173

π_i – an aromatic ring system is named by its first C atom *i*; Cg_i – centroid of the ring *i*.

Table S5. Interactions π-π in $\mathbf{Au_{13}}$**-c**

$\pi_i \cdots \pi_j$	$d(Cg_i \cdots Cg_j)$, Å	α, °	β, °	γ, °	$Cg_{i\perp}$, Å	$Cg_{j\perp}$, Å	Slippage, Å
$\pi_{1B} \cdots \pi_{21A}$	4.11(1)	11	30.5	28.4	3.613(4)	3.54(1)	2.081
$\pi_{1C} \cdots \pi_{21B}$	3.907(8)	6.3(7)	27.8	30.0	3.385(5)	3.456(7)	1.824
$\pi_{1D} \cdots \pi_{21C}$	3.978(7)	7.5(6)	25.5	31.0	3.411(4)	3.590(5)	1.714
$\pi_{2B} \cdots \pi_{21A}$	4.68(1)	12	40.3	46.8	3.202(4)	3.57(1)	3.025
$\pi_{2C} \cdots \pi_{21B}$	4.415(8)	4.7(7)	39.1	43.7	3.193(5)	3.425(7)	2.786
$\pi_{2D} \cdots \pi_{21C}$	4.430(7)	8.6(6)	35.3	44.0	3.190(4)	3.614(5)	2.562

π_i – an aromatic ring system is named by its first C atom *i*; Cg_i – centroid of the ring *i*; α – a dihedral angle between the planes *i* and *j*; β – an angle between the $\overrightarrow{Cg_i \cdots Cg_j}$ vector and normal to the plane *i*; γ – an angle between the $\overrightarrow{Cg_i \cdots Cg_j}$ vector and normal to the plane *j*; $Cg_{i\perp}$ – a perpendicular distance of Cg_i on the ring *j*; $Cg_{j\perp}$ – a perpendicular distance of Cg_j on the ring *i*; Slippage – a distance between Cg_i and perpendicular projection of Cg_j on the ring *i*.

Table S6. Hydrogen bonding in **Au_{13}-c**

D–H···A	*d*(D–H), Å	*d*(H···A), Å	*d*(D···A), Å	∠(D–H···A), °
O2B–H2B···O6W	0.84	1.91	2.70(5)	156
O2D–H2D···O3B^{i}	0.84	1.64	2.45(2)	163
O4A–H4A···O1B^{i}	0.84	1.88	2.70(3)	164
O4B–H4B···O7W	0.84	1.97	2.78(3)	163
O4C–H4C···O2E^{ii}	0.84	1.58	2.40(2)	163
O4D–H4D···O8W	0.84	1.95	2.79(6)	173
C7A–H7A···O3C^{iii}	0.95	2.24	2.96(2)	132
C7C–H7C···O7W^{iii}	0.95	2.52	3.34(2)	144
C25B–H25B···O4B^{iii}	0.95	2.57	3.44(2)	153
O1A···O3W			3.00(4)	
O1A···O6A			2.66(4)	
O1B···O5W			2.93(7)	
O1B···O4A^{ii}			2.70(3)	
O1C···O1W^{iv}			2.65(3)	
O1E···O4C^{i}			3.02(3)	
O2A···O2W			2.91(6)	
O2A···O5A			2.98(4)	
O2B···O6W			2.70(5)	
O2D···O3B^{i}			2.45(2)	
O2D···O7W^{i}			2.76(2)	
O2E···O4C^{i}			2.40(2)	
O3B···O2D^{v}			2.45(2)	
O3D···O5W^{i}			2.94(6)	
O3E···O1W^{i}			2.65(3)	
O4A···O7A			2.77(6)	
O4A···O8A			2.65(6)	
O4A···O1B^{i}			2.70(3)	
O4B···O7W			2.78(3)	
O4C···O1E^{ii}			3.02(3)	
O4C···O2E^{ii}			2.40(2)	
O4D···O8W			2.79(6)	
O4E···O6A^{i}			2.76(3)	
O6A···O4E^{v}			2.76(3)	
O7A···O4A			2.77(6)	
O7A···O8W^{vi}			2.82(7)	
O8A···O4A			2.65(6)	
O8A···O4W			2.70(8)	

O1W···O1C^{vi}	2.65(3)
O1W···O3E^{v}	2.65(3)
O2W···O2A	2.91(6)
O4W···O3W	2.9(1)
O4W···O8A	2.70(8)
O5W···O1B	2.93(7)
O5W···O3D^{v}	2.94(6)
O6W···O2B	2.70(5)
O7W···O4B	2.78(3)
O7W···O2D^{v}	2.76(2)
O8W···O4D	2.79(6)
O8W···O7A^{iv}	2.82(7)

Symmetry code: (i) = -1/2+*x*,1/2-*y*,1/2+*z*; (ii) = -1/2+*x*,1/2-*y*,-1/2+*z*; (iii) = 3/2-*x*,-1/2+*y*,1/2-*z*; (iv) = -1+x,y,z; (v) = 1/2+x,1/2-y,-1/2+z; (vi) = 1+x,y,z.

Table S7: Comparison of water-soluble Au NCs applied in cell-imaging.

Material	**PLQY(H_2O)**	**Decay time (H_2O)**	**Emission**	**Reference**
DHLA–AuNCs	0.6%	(442±13) to (656±10) ns (taken up by cells)	700 nm	small 2011, 7, No. 18, 2614–2620
DPA-capped Au NCs	1.3%	-	610 nm	Nanoscale, 2011, 3, 2009–2014
PBS-Au NCs	-	540 ns	710 nm	Angew. Chem. Int. Ed. 2013, 52, 11154–11157
8-Mercapto-9-propyladenin Au NCs	-	330 nm	510 nm	ACS Appl. Mater. Inter., 2014, 6, 2185-2191.
BSA-Au NCs	-	>100 ns	640 nm	J. Phys. Chem. C 2014, 118, 22339−22346
BSA-Au NCs	-	1.5 μs	470 nm	Nanoscale, 2014, 6, 2594–2597
Lysozymes-Au NCs	-	2.3 ns	515 nm	ChemPhysChem 2016, 17, 253–259
RNase-A@Au NCs	1.9%	-	1050 nm	Angew. Chem. Int. Ed. 2020, 59, 22431–22435
PDMAEMA-AuNCs	3.5%	-	792 nm	Angew. Chem., Int. Ed. , 2023, e202312679.
Au_{13} NC	-	-	650 nm	Nano Res. 2020, 13: 1908–1911
Au_{13}-c cluster	12.6%	792 ns	710 nm	This work
Au_{13}-PEG	8.3%	-	750 nm	This work

DHLA: Dihydrolipoic Acid; DPA: D-penicillamine; PBS: phosphate-buffered saline; BSA: bovine serum albumin; RNase: Ribonuclease-A; PDMAEMA: poly[2(dimethylamino)ethyl methacrylate]

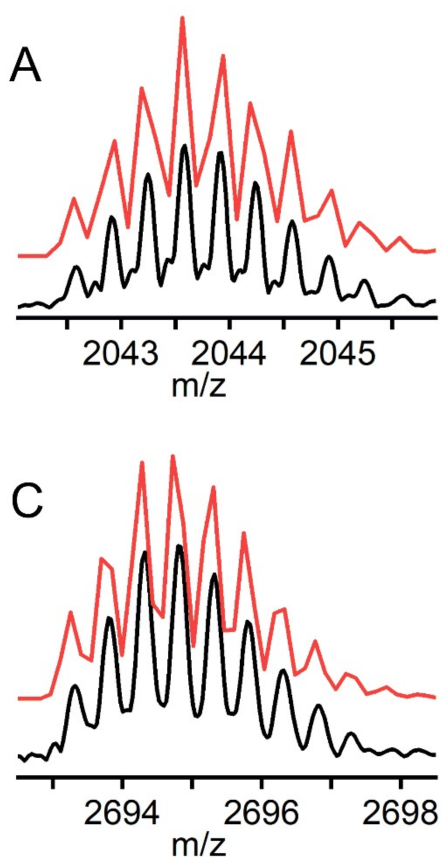

Figure S8. Simulated (red curve) and experimental (black curve) isotope distribution patterns of FTICR-MS of crude reaction mixture dissolved in DMF. (A) $H_{12}[Au_{13}\text{-c+Au(NHC)Cl}]^{3+}$, (B) $H_8[Au_{13}\text{-c(NHC)}_4Cl_3Au_1H_5]^{2+}$, (C) $H_{10}[Au_{13}\text{-c+Cl}]^{2+}$, (D) $H_{10}[Au_{13}\text{-c+AuCl}_2]^{2+}$.

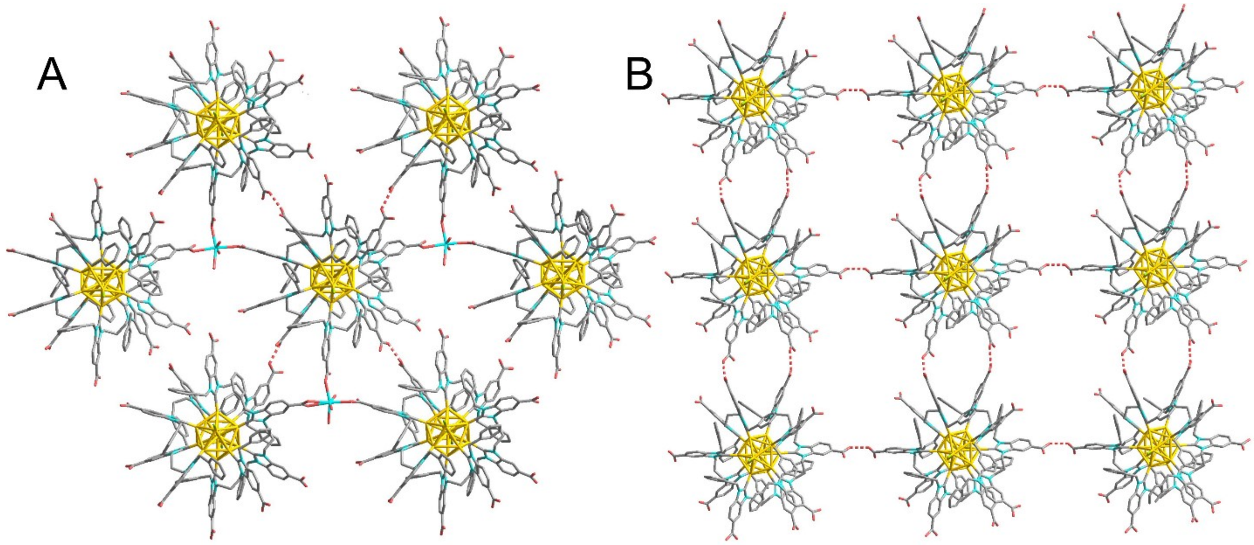

Figure S9. Hydrogen bonds and connections between neigh-boring Au_{13}-c clusters. (A) Crystal of Au_{13}-c cluster; (B) Modified crystallization of Au_{13}-c cluster. Color codes: gold, Au; blue, Na; light green, Cl; aqua, N; light red, O; grey, C and rose, H. Other hydrogen atoms were omitted for clarity.

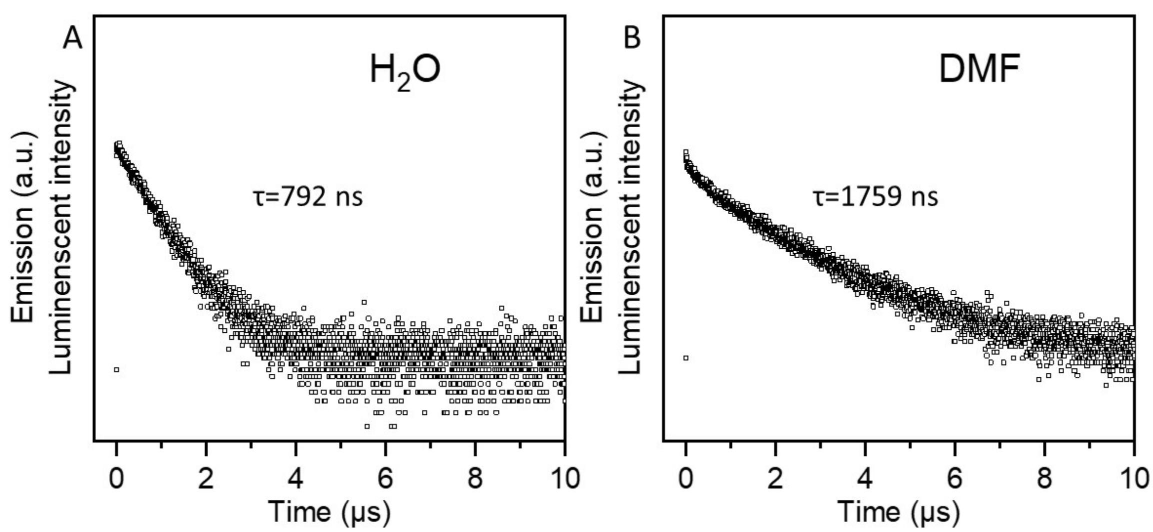

Figure S10. Luminescent decay curve of Au_{13}-c cluster at room temperature. (A) Dissolved in water (pH=14); (B) Dispersed in DMF.

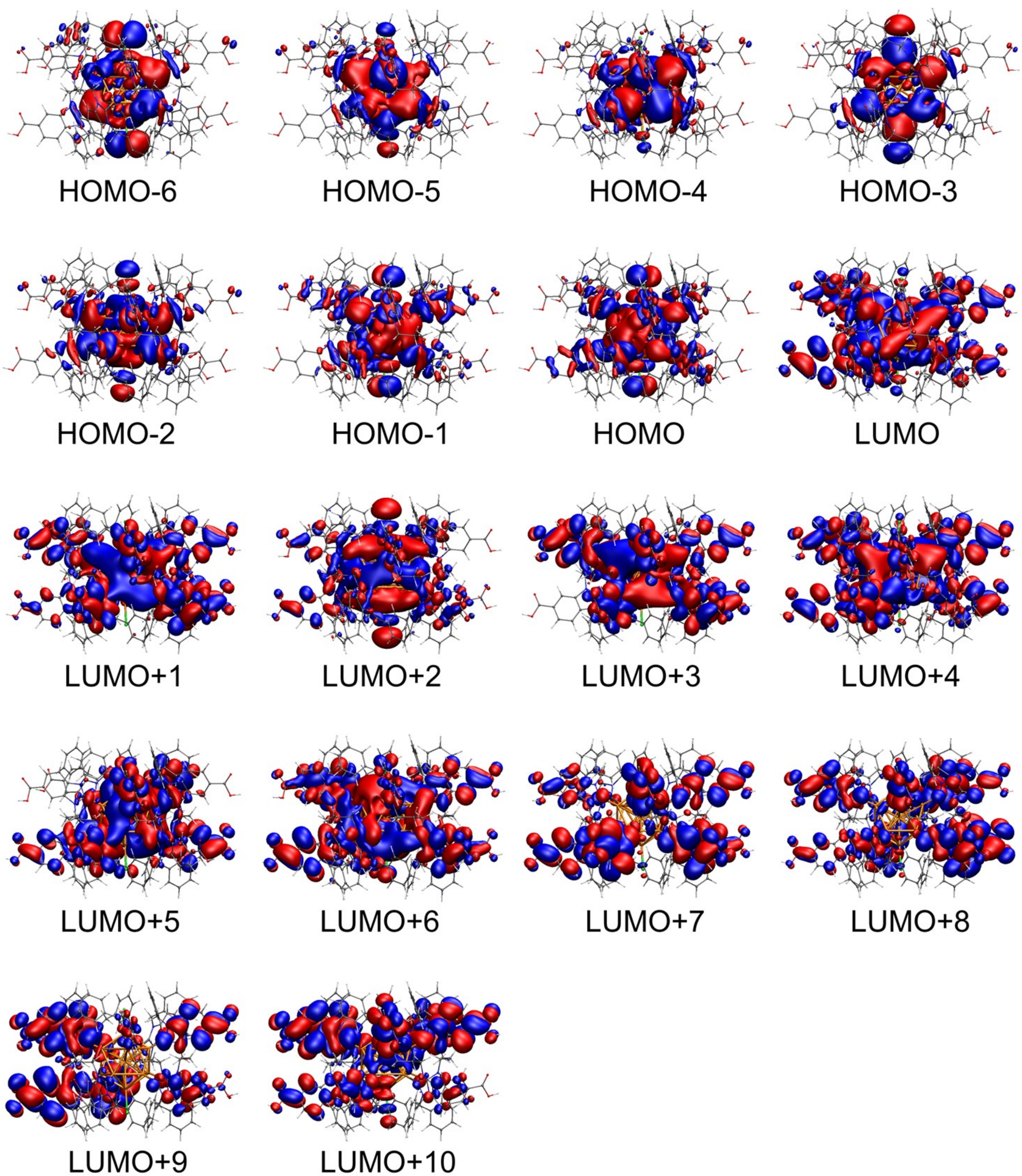

Figure S11. Visualizations of the electron states of the $H_{10}[Au_{13}(\text{bi-NHC carboxyl})_5Cl_2]^{3+}$ cluster from HOMO-6 to LUMO+10. Colors of atoms: Au: orange, C: gray, H: white, Cl: green, N: blue, O: red.

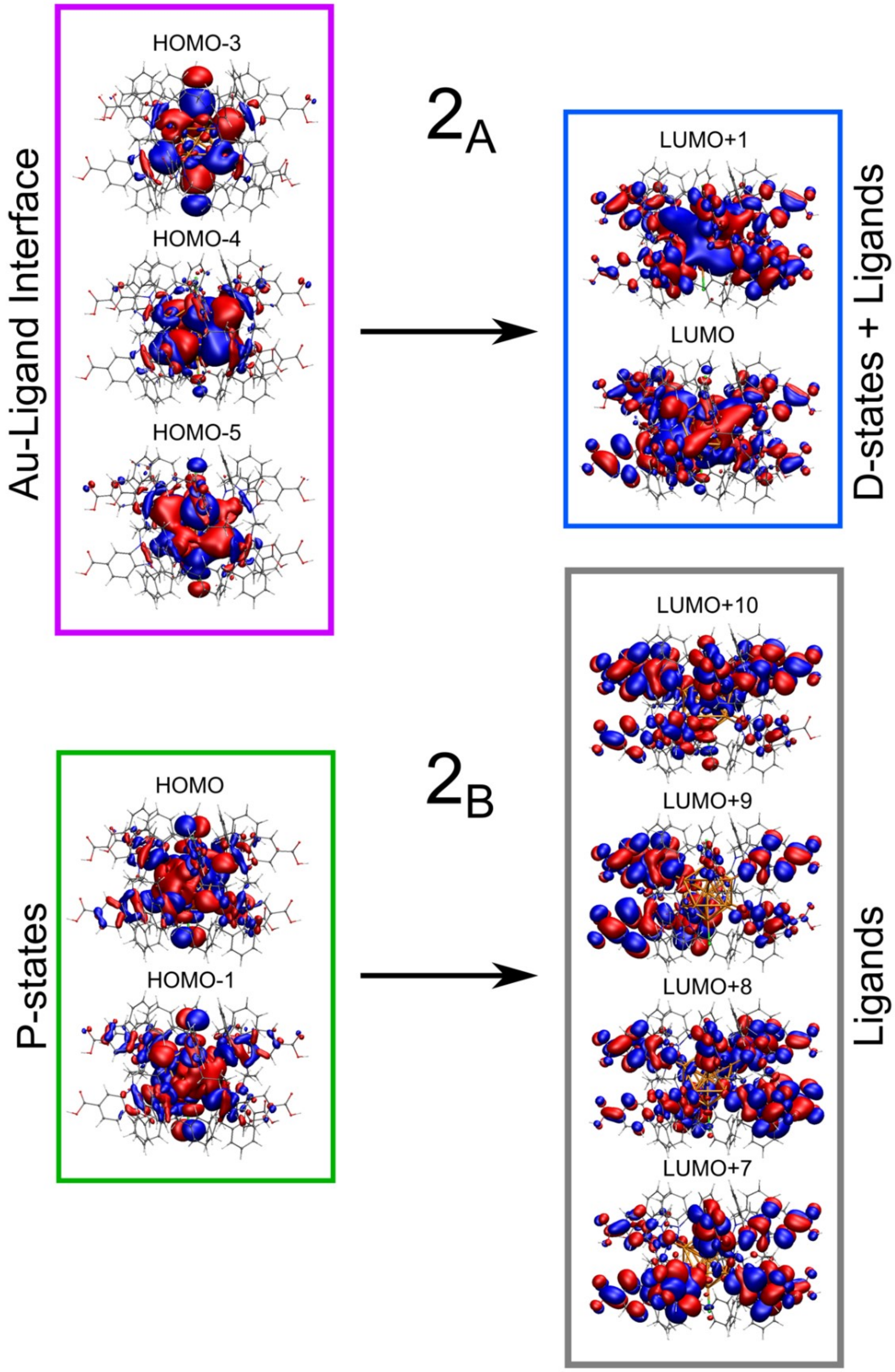

Figure S12. The two main transition contributions of the peak 2 (see figure 3) shown with the visualized electron states. Color coding in rectangular frames follows the colors used for the angular momenta in the PDOS analysis of Figures 3. Colors of atoms: Au: orange, C: gray, H: white, Cl: green, N: blue, O: red.

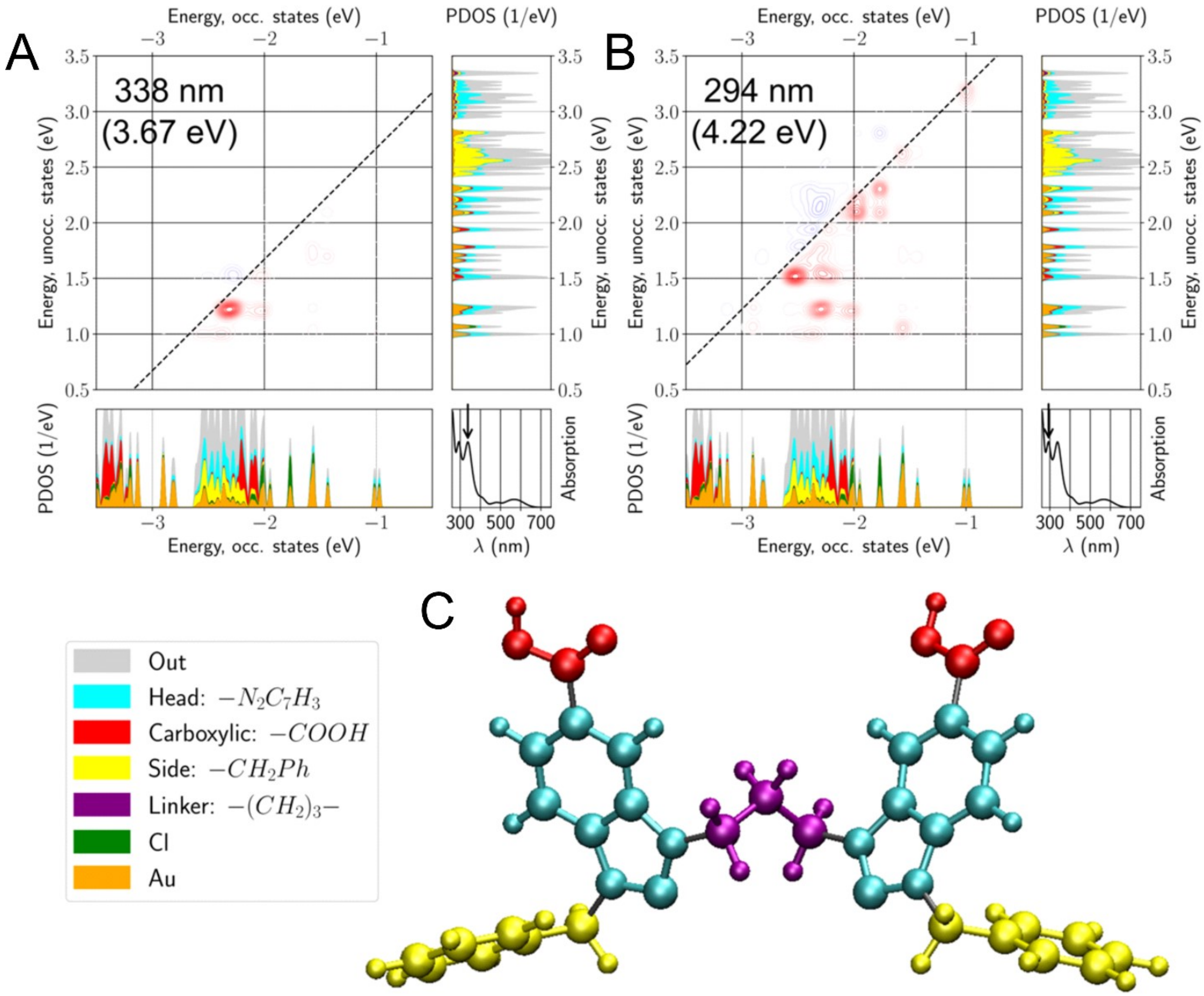

Figure S13. (A)–(B) the same as the DTCM analysis shown in the main text Fig. 3 for the peaks 3 and 4 but plotted using the atom projected density of states. The contributions from different parts of the cluster in atom based PDOS are separated by colors: Au: orange, Cl: green and for carbene ligands: head groups: cyan, carboxylic acid groups: red, side groups: yellow, linker groups: purple. The same colors and structure decomposition are used in the visualization of the bidentate NHC ligand structure in C).

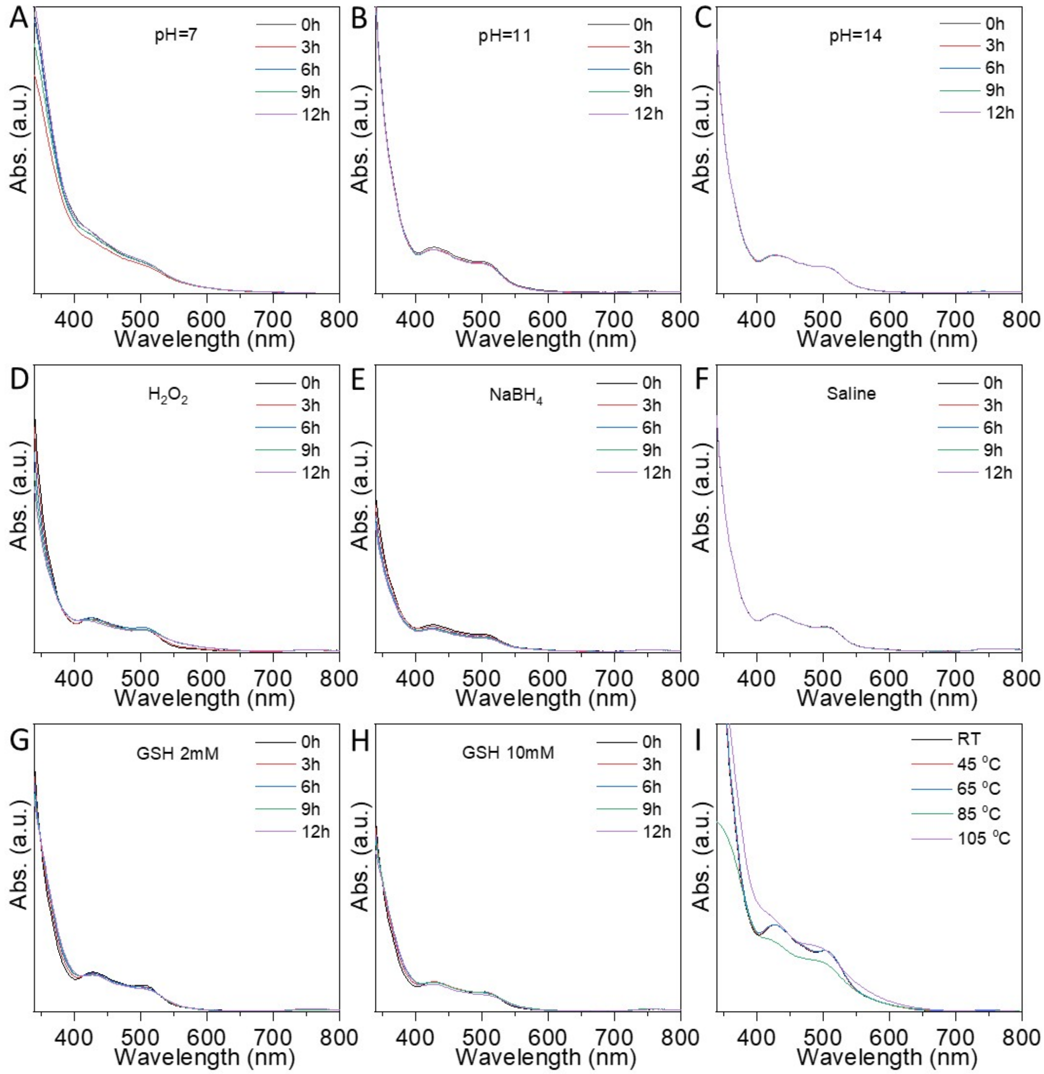

Figure S14. UV-Vis track of Au_{13}-c cluster under a wide range of pHs, red-ox conditions, bio-related environments, and temperatures. (A) pH=7; (B) pH=11; (C) pH=14; (D) H_2O_2; (E) $NaBH_4$; (F) Saline; (G) GSH=2 mM; (H) GSH=10 mM; (I) temperature from RT to 105 ºC.

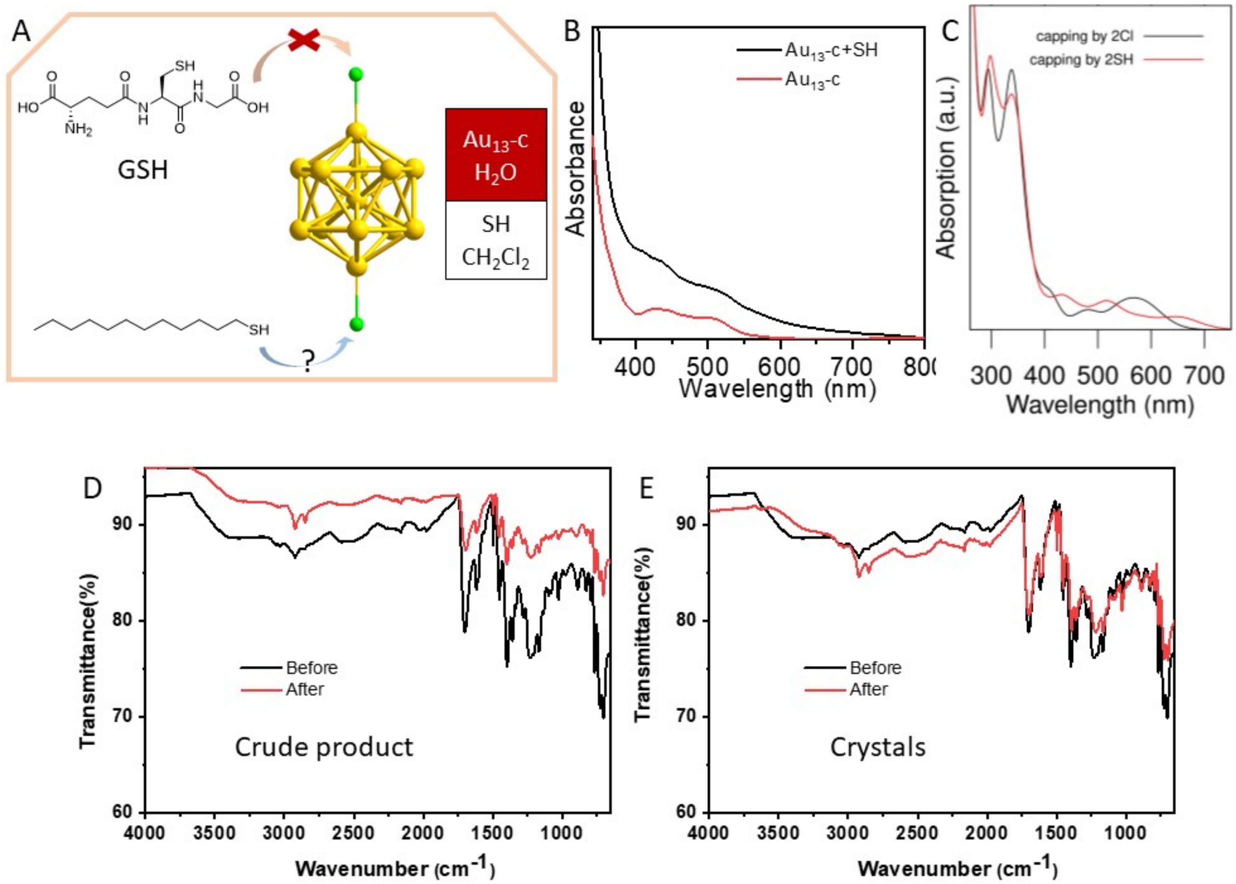

Figure S15. (A) SH replace experiment; (B) Experimental UV-Vis spectra before and after replacement after washing with DCM; (C) Calculated UV-Vis spectra between Au_{13}-c cluster with 2 Cl atoms or SH; (D) IR spectra of replace experiment before and after using the crude product of Au_{13}-c cluster; (E) IR spectra of replace experiment before and after using the crystals of Au_{13}-c cluster.

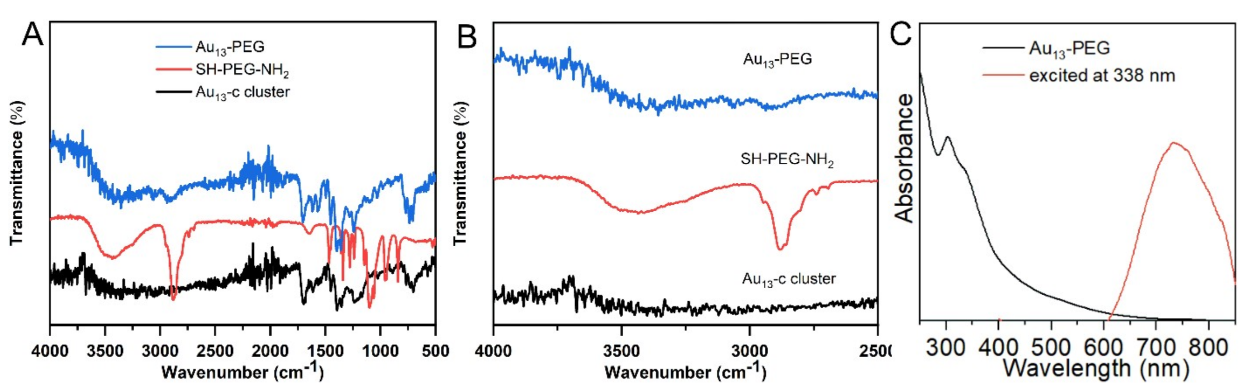

Figure S16. IR spectra of SH-PEG-NH_2, Au_{13}-c cluster and Au_{13}-PEG. (A) The IR spectrum with range from 4000 to 500 cm^{-1}; (B) The IR spectrum with range from 4000 to 2500 cm^{-1}; (C) UV-Vis and emission of Au_{13}-PEG.

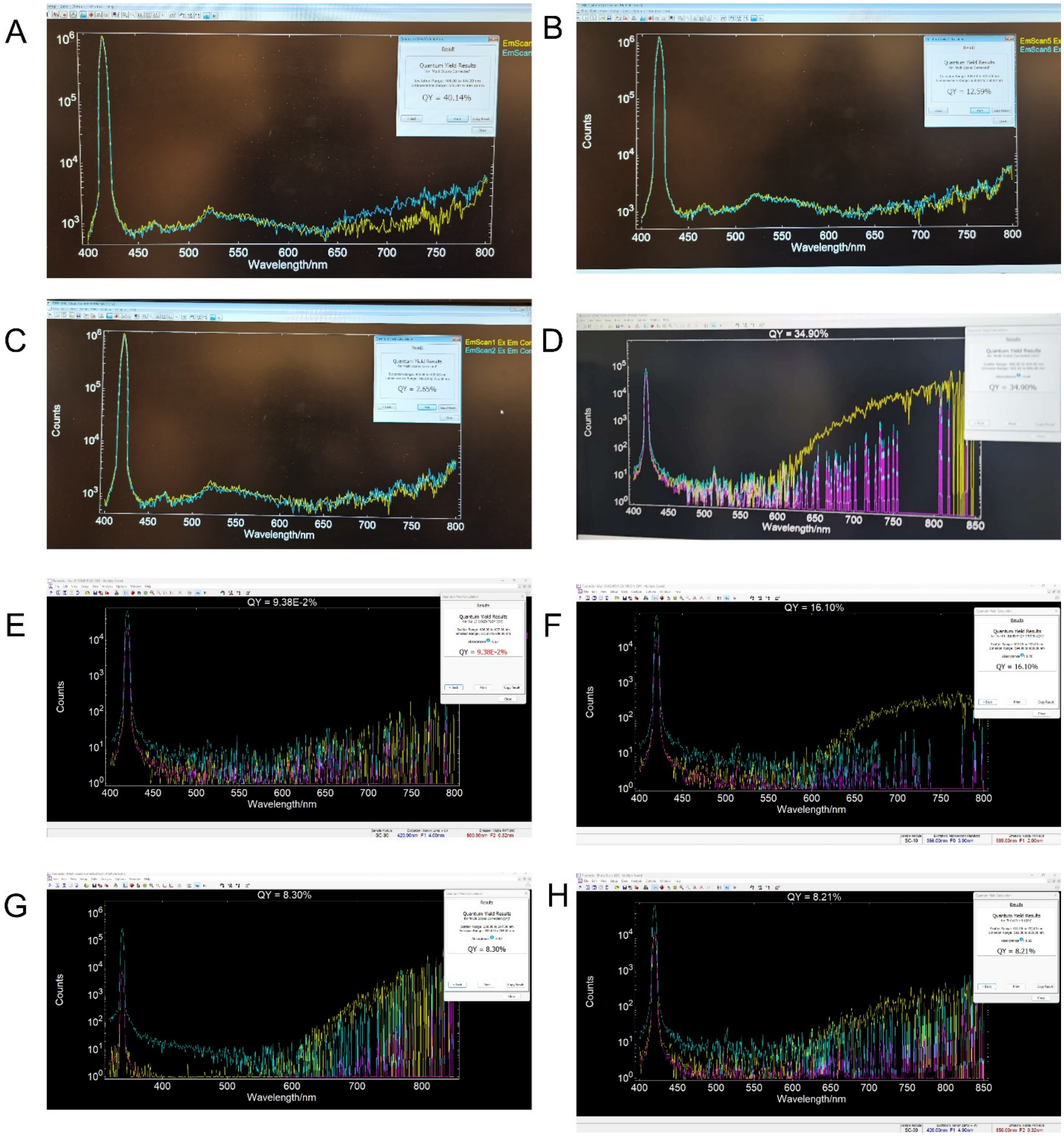

Figure S17. PLQY tests of Au_{13}-c, Au_{13} clusters and Au_{13}-PEG. (A) Au_{13}-c cluster dissolved in DMF; (B) Au_{13}-c cluster dispersed in water; (C) Au_{13}-c cluster dissolved in an aqueous NaOH solution (pH=14); (D) Modified crystals of Au_{13}-c cluster; (E) Crystals of Au_{13} cluster; (F) Au_{13} cluster dissolved in DMF; (G) Au_{13}-PEG dissolved in water; (H) Crystal of Au_{13}-c cluster.

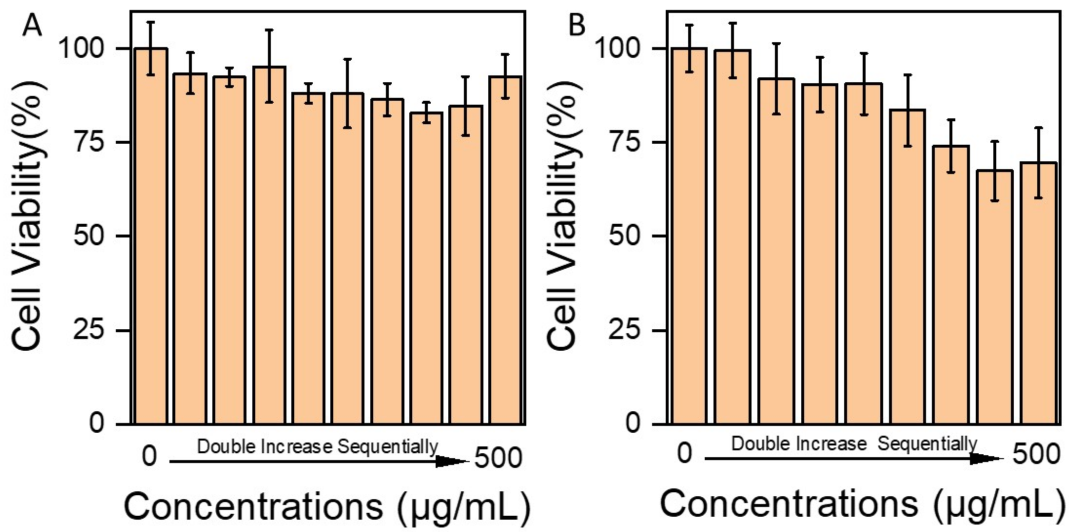

Figure S18. In vitro cytotoxicity of Au_{13}-PEG by MTT assay. The viability of (A) 4T1 cells and (B) L929 cells after culturing in different concentrations of the cluster (0-500 μg/mL) at 37 °C for 12h. The concentrations are from 0, 4.5, 9, 18, 36, 62.5, 125, 250, and finally to 500 μg/mL.

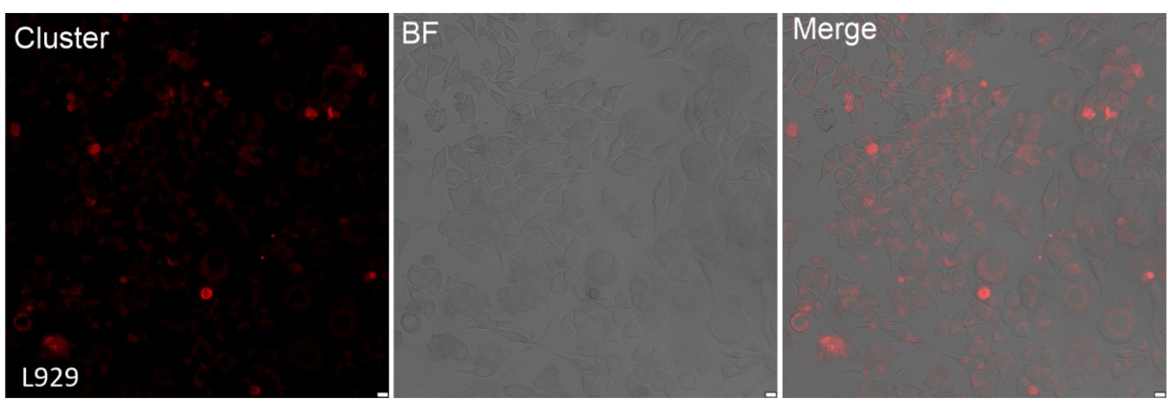

Figure S19. Confocal luminescence microscopic images of the pretreated L929 cells incubated for 24 h. Scale bar = 10 μm.

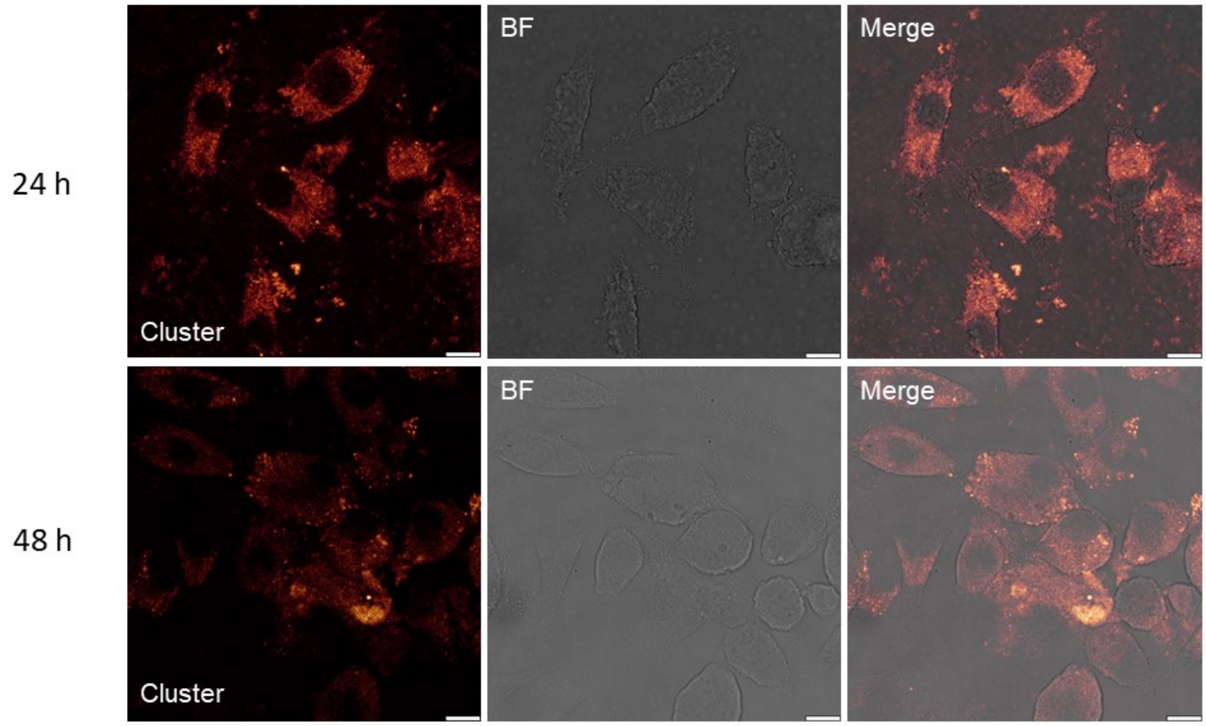

Figure S20. Confocal fluorescence images of Au_{13}-PEG; BF; merge of L929 cells. Scale bar = 10 µm.

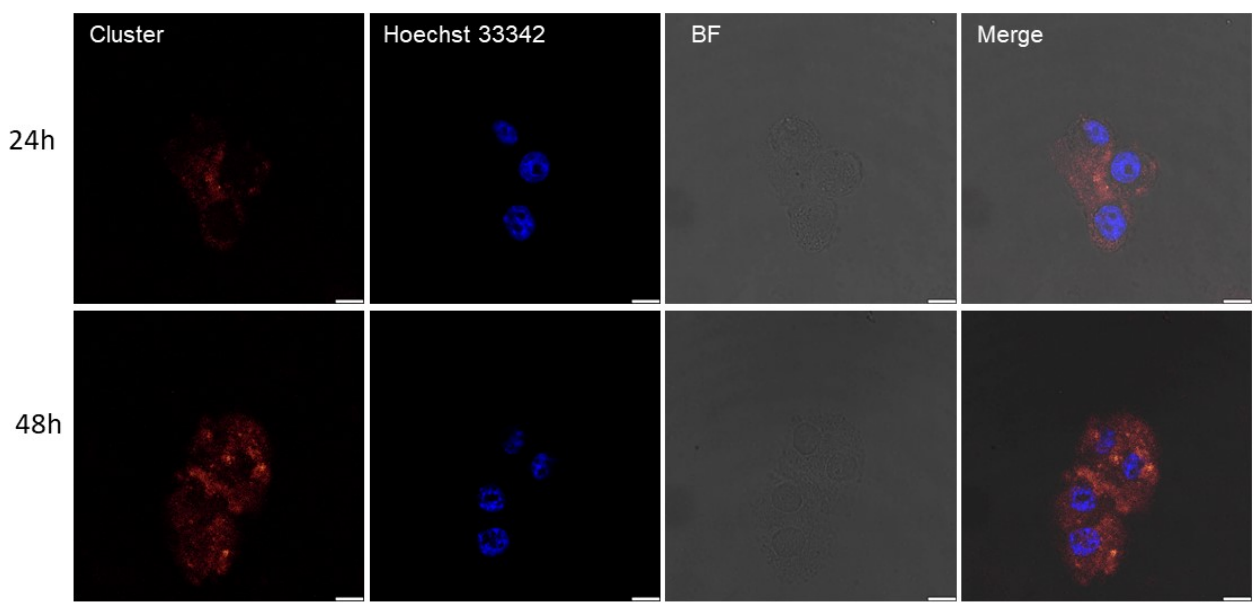

Figure S21. Confocal fluorescence images of 4T1 cells after co-incubating with Au_{13}-PEG (75 µg/mL) for 24 and 48 h (in cluster, Hoechst 33342 and BF channels severally). Scale bar = 10 µm.

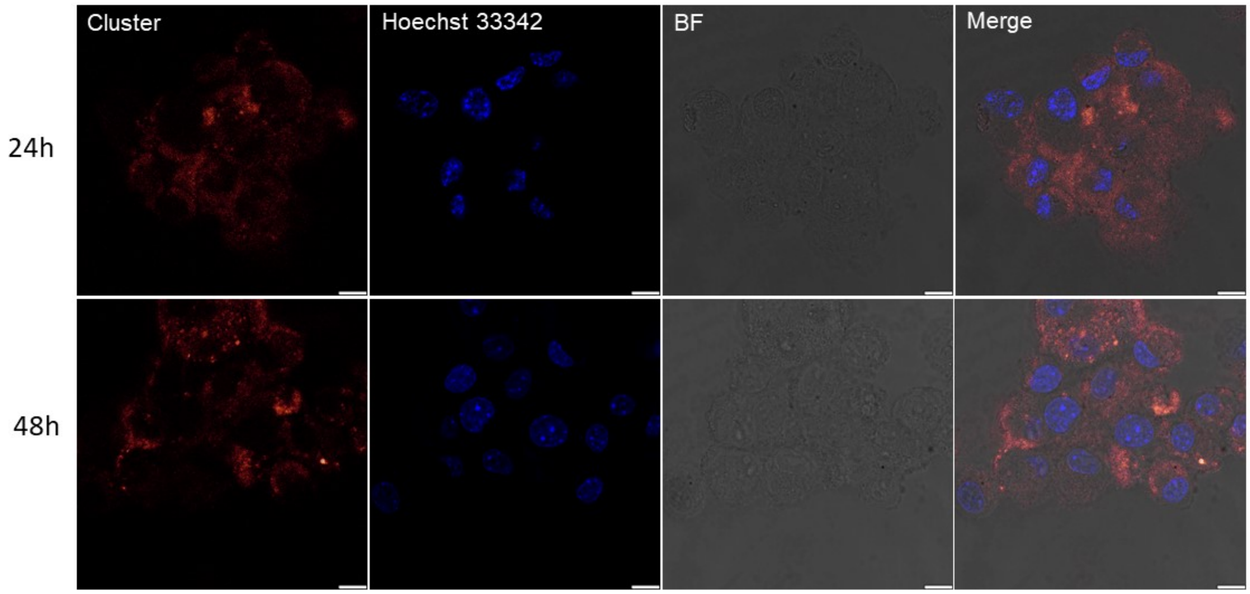

Figure S22. Confocal fluorescence images of L929 cells after co-incubating with Au_{13}-PEG (75 μg/mL) for 24 and 48 h (in cluster, Hoechst 33342 and BF channels severally). Scale bar = 10 μm.

Reference

[1] Yamamoto, Y.; Nishina, N., Gold-Catalyzed Intermolecular Hydroamination of Allenes: First Example of the Use of an Aliphatic Amine in Hydroamination. *Synlett* **2007**, 1767-1770.

[2] Barnard, P. J.; Baker, M. V.; Berners-Price, S. J.; Skelton, B. W.; White, A. H. "Dinuclear gold(I) complexes of bridging bidentate carbene ligands: synthesis, structure and spectroscopic characterisation." *Dalton Trans*: **2004**, 1038-1047.

[3] Salorinne, K.; Man, R. W. Y.; Li, C. H.; Taki, M.; Nam-bo, M.; Crudden, C. M. Water-Soluble N-Heterocyclic Carbene-Protected Gold Nanoparticles: Size-Controlled Synthesis, Stability, and Optical Properties. *Angew. Chem., Int. Ed. Engl.* **2017,** 56, 6198–6202.

[4] a. Bruker AXS Inc, Madison, Wisconsin, USA, 2018; b. empirical absorption correction program. Sheldrick, G.M. Bruker ASX Inc, Madison, Wisconsin, USA, 2002; c. Bruker AXS Inc, Madison, Wisconsin, USA, 2018

[5] Sheldrick, G. M., Phase annealing in SHELX-90 - direct methods for larger structures. *Acta Cryst. A.* **1990,** 46, 467-473.

[6] Sheldrick, G. M., Crystal structure refinement with SHELXL. *Acta Cryst. C.* **2015,** 71, 3-8.

[7] Dolomanov, O. V., Bourhis, L. J., Gildea, R. J., Howard, J. A. K., and Puschmann, H. OLEX2: a complete structure solution, refinement and analysis program. *J Appl Cryst* **2009,** 42, 339-341.

[8] P. van der Sluis & A.L. Spek. BYPASS: an effective method for the refinement of crystal structures containing disordered solvent regions. *Acta Cryst*. **2019,** A46, 194-201.

[9] Enkovaara, J. et al. Electronic structure calculations with GPAW: a real-space implementation of the projector augmented-wave method. *J. Phys. Condens. Matter* **2010,** 22, 253202.

[10] Perdew, J. P.; Burke, K.; Ernzerhof, M. Generalized gradient approximation made simple. Phys. *Rev. Lett.* **1996,** 77, 3865–3868.

[11] Walter, M.; Akola, J.; Lopez-Acevedo, O.; Jadzinsky, P. D.; Calero, G.; Ackerson, C. J.; Whetten, R. L.; Grönbeck, H.; Häkkinen, H. A unifiedview of ligand-protected gold clusters as superatom complexes, *Proc. Natl. Acad. Sci. U.S.A.* **2008**, *105*, 9157–9162.

[12] Walter, M. et al. Time-dependent density-functional theory in the projector augmented-wave method. *J. Chem. Phys.* **2008**, *128*, 244101.

[13] S. Malola, L. Lehtovaara, J. Enkovaara, H. Häkkinen, Birth of the Localized Surface Plasmon Resonance in Monolayer-Protected Gold Nanoclusters. *ACS Nano* **2013**, *7*, 10263-10270

[14] Shen, H.; Xiang, S. J.; Xu, Z.; Liu, C.; Li, X. H.; Sun, C. F.; Lin, S. C.; Teo, B. K.; Zheng, N. F., Superatomic Au_{13} Clusters Ligated by Different N-heterocyclic Carbenes and Their Ligand-dependent Catalysis, Photoluminescence, and Proton Sensitivity. *Nano. Res.* **2020**, 13, 1908-1911.

[15] Yi, H.; Osten, K. M.; Levchenko, T. I.; Veinot, A. J.; Aramaki, Y.; Ooi, T.; Nambo, M.; Crudden, C. M., Synthesis and enantioseparation of chiral Au_{13} nanoclusters protected by bis-N-heterocyclic carbene ligands. *Chem. Sci.* **2021**, 12, 10436-10440.

[16] Luo, P.; Bai, S.; Wang, X.; Zhao, J.; Yan, Z. N.; Han, Y. F.; Zang, S. Q.; Mak, T. C. W., Tuning the Magic Sizes and Optical Properties of Atomically Precise Bidentate N-Heterocyclic Carbene-Protected Gold Nanoclusters via Subtle Change of N-Substituents. *Adv. Optical Mater.* **2021**, 9, 2001936-2001941.